Available online at www.sciencedirect.com
ScienceDirect
Journal of Pharmaceutical and Biomedical Analysis 43 (2007) 1692–1699
JOURNAL OF PHARMACEUTICAL AND BIOMEDICAL ANALYSIS
www.elsevier.com/locate/jpba

Characterization of polymethoxylated flavones in *Fructus aurantii* by liquid chromatography with atmospheric pressure chemical ionization combined with tandem mass spectrometry

Da-Yong Zhou [a], De-Liang Chen [b], Qing Xu [a], Xing-Ya Xue [a], Fei-Fang Zhang [a], Xin-Miao Liang [a,*]

[a] *Dalian Institute of Chemical Physics, Chinese Academy of Sciences, Dalian 116023, PR China*
[b] *Division of Cardiology, Department of Internal Medicine, Wuhan University, ZhongNan Hospital, Wuhan, Hubei Province 430071, PR China*

Received 31 August 2006; received in revised form 20 December 2006; accepted 28 December 2006
Available online 10 January 2007

Abstract

Atmospheric pressure chemical ionization mass spectrometry (APCI-MS) was operated in positive mode (PI) to characterize polymethoxylated flavonoids (PMFs) through its specific radical cations by collision-induced dissociation (CID). The fragments of $[M+H-n\times 15]^+$ produced by loss of one or more methyl group from the protonated molecule, as well as $[M+H-29]^+$, $[M+H-31]^+$, $[M+H-33]^+$, $[M+H-43]^+$, $[M+H-46]^+$, and $[M+H-61]^+$ fragment ions were detected, which were diagnostic for the polymethoxylated species, and could be adopted to form the multiple MS (MS^n) "fingerprint" of PMFs. Based on this "fingerprint", 29 PMFs were screened out from extracts of *Fructus aurantii*, among which two of them were identified as sinensetin and tangeretin. It was proved that the PI was suitable for structural characterization of PMFs by APCI-MS^n.

Keywords: LC–MS; CID MS/MS; Characterization; PMFs; *Fructus aurantii*

1. Introduction

Fructus aurantii (*Zhi qiao*) is from the dried, mature fruit of *Citrus aurantium* L. (immature fruit named *Zhishi*). As an important traditional Chinese medicine (TCM), it showed bioactivities of anti-tumor [1], anti-hypertension [2], anti-shock [3], etc. Our preliminary studies indicated that main bioactive constituents of *F. aurantii* were flavonoids, especially some *O*-diglycosyl flavanones [4] and PMFs. Flavonoids are one of the most widespread groups of secondary plant metabolites. It is estimated that about 2% of all carbon phytosynthesized by plants is converted into flavonoids or closely related compounds [5]. PMFs constitute a special group of flavonoids that is present in certain citrus species. PMFs possess important biochemical and physiological effects, including anti-allergic [6], anti-inflammatory [7], anti-oxidant [8], anti-proliferative [9,10], anti-bacterial [11] activities and effects to mammalian metabolism [12]. Therefore, it is necessary to identify the PMFs in *F. aurantii*, which can give wide outlook on the applications of this Chinese herb.

^1H and ^{13}C NMR techniques are preferred for structural assignment, however, in phytochemical analysis, high amount of PMFs is not always easily be isolated so that alternative techniques have to be employed. The recent progress in soft ionization techniques, especially APCI and electrospray ionization (ESI) source MS have emerged as highly useful mass spectrometric method used in phytochemical studies that allow the direct conjugation with LC [13–17]. These soft ionization techniques favorably produce protonated or deprotonated molecule ions with little fragmentation that can be used for structural analysis. So, CID is used to obtain fragmentation of structural relevance. The tandem mass spectrometric fragmentation behaviors of flavonoids have been investigated extensively, and thus, allow the identification of unknown compounds even when reference standards are unavailable.

Therefore, in the purpose of phytochemical screening and structural characterization of PMFs in *F. aurantii*, a LC–MS and CID MS/MS experiment was adopted to investigate the specific

* Corresponding author. Tel.: +86 411 84379519; fax: +86 411 84379539.
E-mail address: liangxm@dicp.ac.cn (X.-M. Liang).

0731-7085/$ – see front matter © 2007 Elsevier B.V. All rights reserved.
doi:10.1016/j.jpba.2006.12.032

fragment patterns of two PMFs sinensetin and tangeretin and its application in the identification of PMFs compounds from the extract of *F. aurantii.* APCI was preferred in the present experiments because the PMFs compounds in the *F. aurantii* samples were favorably analyzed with this ionization mode.

2. Materials and methods

2.1. Standards and reagents

PMFs standards, sinensetin (SIN, 3′,4′,5,6,7-pentamethoxyflavone, MW 372) was purchased from Meryer (Sweden); tangeretin (TAN, 4′,5,6,7,8-pentamethoxyflavone, MW 372) was purchased from Xiantong Times (China). The standards were diluted in acetonitrile to form a PMFs stock solution of 1 mg/mL, and this solution was then diluted further in acetonitrile to form a PMFs work solution at 100 ng/mL before LC–MS analysis. The following agents were in HPLC grade: acetonitrile purchased from Merck (Germany), formic acid purchased from J&K CHEMICA (USA), ethanol, methanol and ethyl acetate purchased from Yuwang (China). Reverse osmosis Milli-Q water (18.2 MΩ) (Millipore, USA) was used for all solutions and dilutions.

2.2. Instrumentation

An Agilent 1100 Series LC/MSD Trap XCT (Agilent, USA) with a photodiode-array detector set at 300 nm (monitoring length). Chromatographic conditions were as follow: column, Hypersil ODS2 C_{18} (Elite, China), 250 mm × 4.6 mm, 5 μm; eluent: (A) water–formic acid (100:0.5, v/v), (B) acetonitrile–formic acid (100:0.5, v/v). The linear gradient was: 0–45 min, 20–60% B. The flow-rate was 1 mL/min and the column temperature was 30 °C. Ten μL of sample solution were injected for analysis.

APCI mass spectra were acquired in PI. Nitrogen was used as the nebulizing gas at 60 psi and as drying gas at flow rate of 7 L/min and temperature of 350 °C. The vaporizer temperature was set at 400 °C. Ions were obtained in the range of *m/z* 100–600. MS^n spectra was obtained by auto-MS^4 mode (the product-ion of base peak was selected as precursor ion for next stage MS automatically), the fragmentation amplitude (FA) was set at 1, 1.5, 2, 2.5, 3, 3.5 and 4 V (SmartFrag: 30–200%), respectively in each time of repeated experiments to obtain various fragmentation for structural elucidation and the MS^n isolation width was 4.0 *m/z*. The LC flow was directed into the mass spectrometer without stream splitting.

2.3. Plant material and sample preparation

F. aurantii were collected from Kai County, Chongqing city, China. The herb was authenticated by Institute of Medication, Xiyuan Hospital of China Academy of Traditional Chinese Medicine. The extraction was performed by MaiDiHai Pharmacy Corporation (China). The procedures were as follow: 100 kg herb was grounded into powder and decocted in 1000 L water at 100 °C, 120 min. Then the residue was collected and re-decocted in 1000 L water at 100 °C, 90 min. The decoction in both times were collected and dried by spray drying (percentage of yield was 10). So large amount of herb was used, as we wanted to isolate some micro-level components from this herb. Then 1.5 kg fine powder of extract was dissolved by 15 L water–ethanol (30:70, v/v). After stirred continuously for 0.5 h, the solution was placed at room temperature for 12 h. The mixture was filtered using filter paper and the filtrate was dried with a rotary evaporator at 60 °C. The residue was dissolved by 1 L water and extracted twice by 5.25 L and 2.25 L ethyl acetate, respectively. The organic layer in both time were collected and combined, then dried with a rotary evaporator at 60 °C.

3. Results and discussion

3.1. MS condition

Our preliminary experiments showed that better response was obtained for some PMFs with APCI in PI, therefore, further experiments were carried out in such mode. The FA was set at different voltages to obtain an optimum degree of fragmentation. The dominant fragments were subsequently isolated automatically and subjected to a second or a third stage of collision (auto-MS^n) in the ion trap to map the sequential fragment routes and provided additional structural information. The collision gas was nominally 1 mTorr helium, which is the standard buffer gas used in ion traps.

3.2. MS^n "fingerprint" of PMFs

In order to identify PMFs from complex matrix, the diagnostic MS "fingerprint" was built up firstly basing on the mass spectra of two commercially PMF standards, TAN and SIN. Through PI-APCI MS, their molecular weights (MWs) were confirmed firstly. Their structural information was obtained by MS^n with optimized FA at 1.5 V.

The MS^n product-ions spectra of protonated TAN were shown in Fig. 1. The main fragment pathways of TAN were proposed in Fig. 2. Upon the first step of CID, the protonated flavones TAN dissociate predominantly via loss of a methyl radical ($CH_3^\bullet$) and formed the radical cation $[M+H-15]^+$ as base peak. This characteristic fragmentation was detected previously in MS analysis of methoxylated flavonoids by several investigators [18]. At the same time, other main fragments, corresponding to the loss of $30(2CH_3^\bullet)$, $61(CO+H_2O+CH_3^\bullet)$, $48(2CH_3^\bullet+H_2O)$, 60, $28(CO)$, $33(H_2O+CH_3^\bullet)$ and $44(CO_2)$ from the protonated molecule were observed too. In MS^3 spectrum of TAN, the radical cation $[M+H-15]^+$ was followed exclusively by a second elimination of methyl radical as dominant dissociation. Other fragments corresponding to the loss of $46(CO+H_2O)$, $33(H_2O+CH_3^\bullet)$, 45, $29(HCO^\bullet)$, $61(CO+H_2O+CH_3^\bullet)$, and 63 from precursor-ion were observed as main dissociation. In MS^4 spectrum of TAN, the dominating fragment was peak corresponding to the loss of $46(CO+H_2O)$, while the cation corresponding to the loss of $15(CH_3^\bullet)$ was observed as secondary fragment. Other fragments, corresponding to the loss of $28(CO)$, $43(CH_3^\bullet+CO)$,

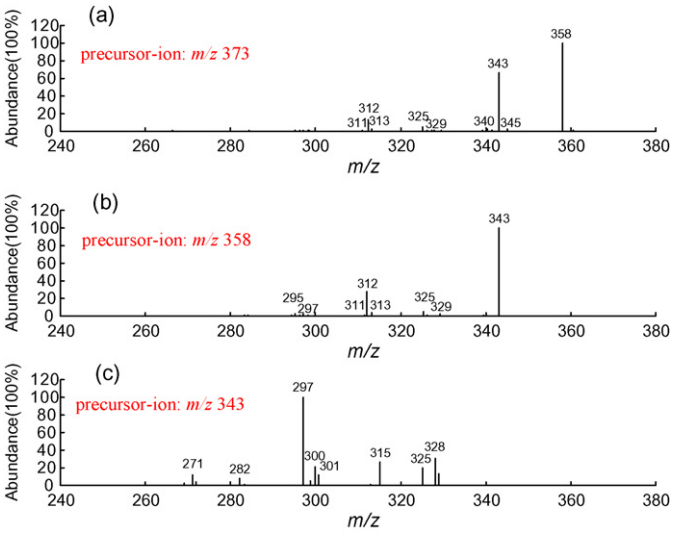

Fig. 1. The CID-MS spectra of TAN: (a) MS^2 spectrum (precursor-ion was 373 ($[M+H]^+$)); (b) MS^3 spectrum (precursor-ion was 358 ($[M+H-15]^+$)); (c) MS^4 spectrum (precursor-ion was 343 ($[M+H-30]^+$)).

18(H_2O), 42(C_2H_2O), 72 and 61($CO+H_2O+CH_3^\bullet$) from precursor-ion were observed as main dissociation.

The MS^n product-ions spectra of protonated SIN were shown in Fig. 3. The MS^2 spectrum of SIN exhibited a fragment loss of 61($CO+H_2O+CH_3^\bullet$) as base peak. Other fragments corresponding to the loss of 15($CH_3^\bullet$), 44(CO_2), 30($2CH_3^\bullet$), 33($H_2O+CH_3^\bullet$), 60, 29($HCO^\bullet$) and 46($CO+H_2O$) from the protonated molecule were observed too. Compared to TAN, the MS^2 spectrum of SIN exhibited two extra fragments corresponding to loss of 16(CH_4) and 14($CH_2^{\bullet\bullet}$) which were diagnostic ions of PMFs (see Fig. 4). In MS^3 spectrum of SIN, the loss of 15 from precursor-ion formed the base peak. Other cations corresponding to the loss of 43($CH_3^\bullet+CO$), 31($CH_3O^\bullet$), 28(CO) and 61($CO+H_2O+CH_3^\bullet$) from precursor-ion were observed as main fragments. At the same time, some low *m/z* fragments such as 151, 155 and 163 were also detected, though the exact structure of them could not be confirmed. No fragment of SIN was observed in MS^4 experiments. The main fragments of SIN and TAN were summarized in Table 1.

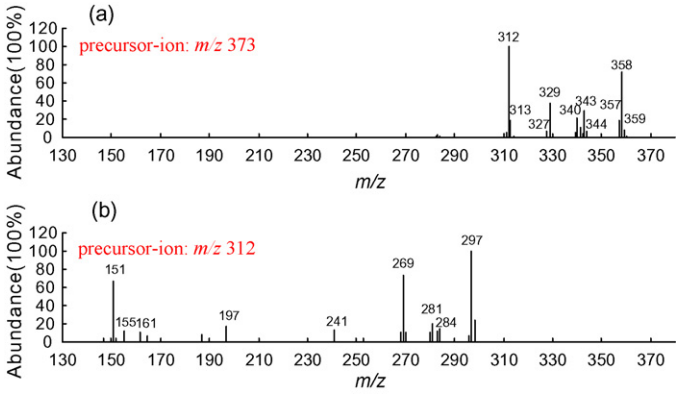

Fig. 3. The CID-MS spectra of SIN: (a) MS^2 spectrum (precursor-ion was 373($[M+H]^+$)); (b) MS^3 spectrum (precursor-ion was 312 ($[M-61+H]^+$)).

Comparing the product-ions spectra of the two isomeric compounds SIN and TAN, similar fragment pathways was showed partly, including the mutual fragmentation from loss of 15, 29, 30, 33, 43, 46, and 61, which formed the characteristic MS^n "fin-

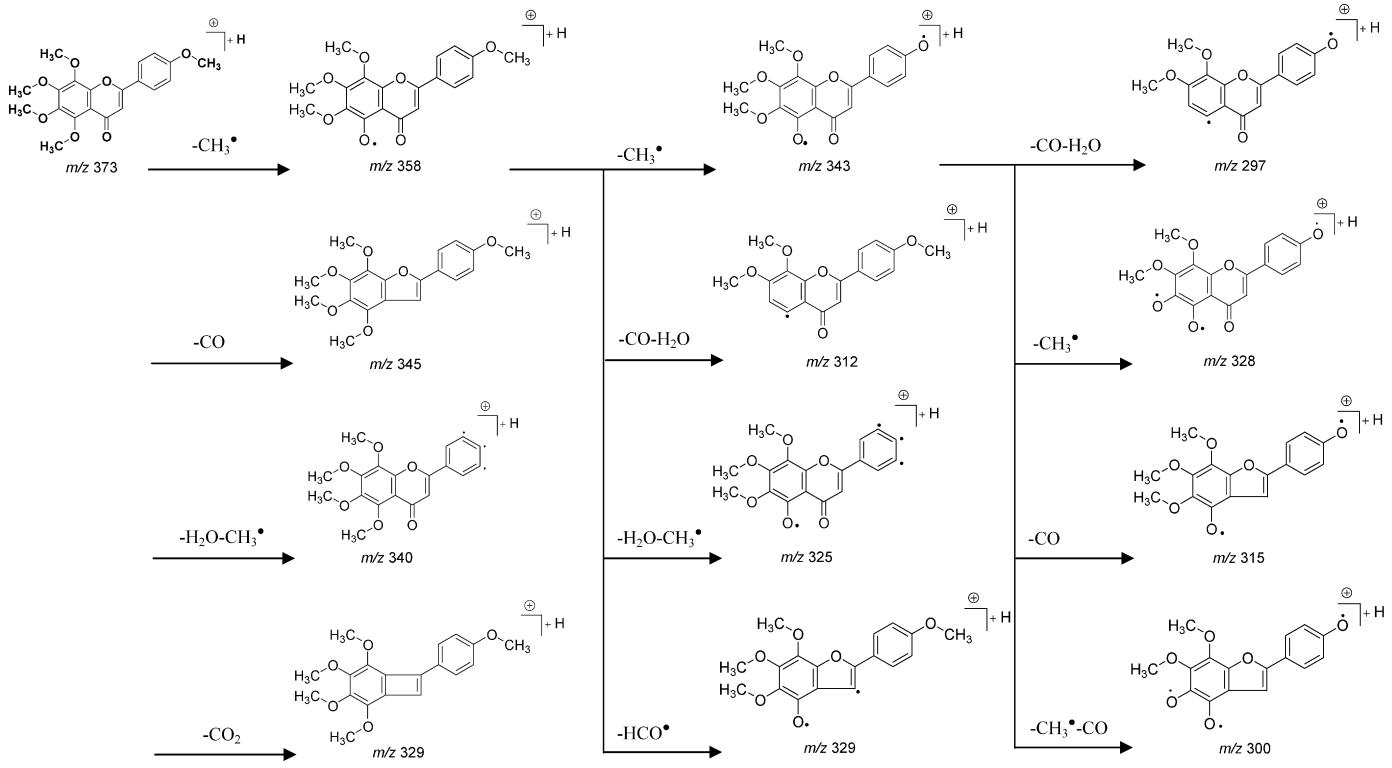

Fig. 2. Proposed mainly characteristic fragmentations from the protonated TAN.

Table 1
CID patterns of protonated SIN and TAN

No.	RT (min)	FA (V)	$[M+H]^+$	MS/MS			MS/MS/MS			MS/MS/MS/MS		
				P-ion (%)	Loss (u)	L-R	P-ion (%)	Loss (u)	L-R	P-ion (%)	Loss (u)	L-R
SIN	26.0	1.5	373	312※(100)	61	$CO+H_2O+CH_3^•$	297(100)	15	$CH_3^•$			
				358(71.8)	15	$CH_3^•$	269(73.3)	43	$CH_3^•+CO$			
				329(37.3)	44	CO_2	281(20.3)	31	$OCH_3^•$			
				343(29.3)	30	$2CH_3^•$	284(14.2)	28	H_2O			
				340(20.9)	33	$H_2O+CH_3^•$	241(12.8)	61	$CO+H_2O+CH_3^•$			
				357(18.6)	16	CH_4	151(67.3)		–			
				313(18.0)	60	–	155(11.4)		–			
				344(6.7)	29	$HCO^•$	161(10.1)		–			
				359(8.5)	14	$CH_2^{••}$						
				327(6.0)	46	$CO+H_2O$						
TAN	34.1	1.5	373	358※(100)	15	$CH_3^•$	343※(100)	15	$CH_3^•$	297(100)	46	$CO+H_2O$
				343(66.9)	30	$2CH_3^•$	312(27.9)	46	$CO+H_2O$	328(30.3)	15	$CH_3^•$
				312(13.2)	61	$CO+H_2O+CH_3^•$	325(5.9)	33	$H_2O+CH_3^•$	315(27.2)	28	CO
				325(5.1)	48	$H_2O+2CH_3^•$	313(3.8)	45	–	300(21.3)	43	$CH_3^•+CO$
				313(2.8)	60	–	329(3.3)	29	$HCO^•$	325(19.8)	18	H_2O
				345(2.7)	28	CO	297(2.9)	61	$CO+H_2O+CH_3^•$	271(12.0)	72	–
				340(2.6)	33	$H_2O+CH_3^•$	295(2.4)	63	–	301(11.3)	42	C_2H_2O
				329(2.0)	44	CO_2			–	282(8.5)	61	$CO+H_2O+CH_3^•$

$[M+H]^+$ represents the m/z of the protonated flavone. P-ion (%) represents the product ions and the relative percentage. The product ions tag with "※" represents precursor-ion for next stage MS. L-R represents the radical of loss.

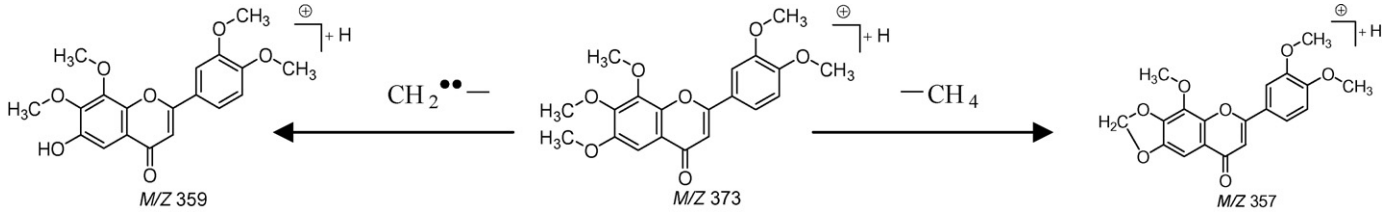

Fig. 4. Proposed characteristic fragmentations corresponding to loss of 14($CH_2^{\bullet}$) and 16(CH_4) from the protonated SIN.

gerprint" that can be applied to screen out similar PMFs in highly complex mixture. Among these diagnostic fragments, the dissociation by loss of 15, 29, 30 and 43 were previously detected as diagnostic fragments also by ESI-MS in characterization of PMFs [18]. The fragments corresponding to the neutral loss of 18, 28 and 44 observed in some of the product-ions spectra were reported before in characterization of flavonoids [19], too.

3.3. Extracted ion chromatogram (EIC) method

The purpose of our study was to screen and characterize PMFs in *F. aurantii* extract. Through standards SIN and TAN, the diagnostic MS^n "fingerprint" of PMFs had been obtained. Then, the candidates of PMFs in *F. aurantii* should be selected by some methods for farther characterization by these "fingerprint". PMFs have the basic aglycone structure and differ in the position and number of methoxyl groups (OCH_3) and/or hydroxyl group (OH) on the A, B and C rings of aglycone. The MW of basic structure of aglycone is 222 u (see Fig. 5), which is increased by 30 or 16 when a methoxyl or hydroxyl group was added. Through this regularity, the MWs of all possible PMFs

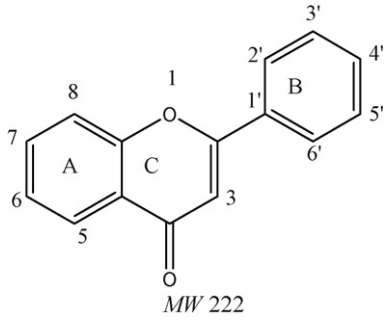

Fig. 5. The basic structure of flavone aglycones.

Table 2
The MWs and structural identification of all possible PMFs be detected in *Fructus aurantii*

No.	Polymethoxylated flavones	The number of methoxyl group (OCH_3)	The number of hydroxyl group (OH)	MW	The tag of peak
1	Tetrahydryoxy-dimethoxyflavone	2	4	346	347(1)
2	Tetrahydryoxy-dimethoxyflavone	2	4	346	347(2)
3	Monohydryoxy-trimethoxyflavone	3	1	328	329
4	Dihydryoxy-trimethoxyflavone	3	2	344	345
5	Tetramethoxyflavone	4	0	342	343(1)
6	Tetramethoxyflavone	4	0	342	343(2)
7	Monohydryoxy-tetramethoxyflavone	4	1	358	359
8	Dihydryoxy-tetramethoxyflavone	4	2	374	375(1)
9	Dihydryoxy -tetramethoxyflavone	4	2	374	375(2)
10	Trihydryoxy-tetramethoxyflavone	4	3	390	391
11	Pentamethoxyflavone	5	0	372	373(1)
12	Pentamethoxyflavone	5	0	372	373(2)
13	Pentamethoxyflavone	5	0	372	373(3)
14	Monohydryoxy-pentmethoxyflavone	5	1	388	389(1)
15	Monohydryoxy-pentmethoxyflavone	5	1	388	389(2)
16	Monohydryoxy-pentmethoxyflavone	5	1	388	389(3)
17	Monohydryoxy-pentmethoxyflavone	5	1	388	389(4)
18	Monohydryoxy-pentmethoxyflavone	5	1	388	389(5)
19	Monohydryoxy-pentmethoxyflavone	5	1	388	389(6)
20	Dihydryoxy-pentmethoxyflavone	5	2	404	405(1)
21	Dihydryoxy-pentmethoxyflavone	5	2	404	405(2)
22	Dihydryoxy-pentmethoxyflavone	5	2	404	405(3)
23	Dihydryoxy-pentmethoxyflavone	5	2	404	405(4)
24	Hexamethoxyflavone	6	0	402	403
25	Monohydroxy-hexamethoxyflavone	6	1	418	419(1)
26	Monohydroxy-hexamethoxyflavone	6	1	418	419(2)
27	Monohydroxy-hexamethoxyflavone	6	1	418	419(3)
28	Monohydroxy-hexamethoxyflavone	6	1	418	419(4)
29	Heptamethoxyflavone	7	0	432	433

Table 3
CID-MS patterns of protonated PMFs in FOE

No.	RT (min)	FA (V)	$[M+H]^+$ (*m/z*)	MS/MS loss (u) (%)	MS/MS/MS loss (u) (%)	MS/MS/MS/MS loss (u) (%)
1	19.4	1.5	347(1)	15※(100), 32(17.6), 20(16.4), 19(14.3), 14(14.3), 17(9.3), 46(9.3), 18(8.0)	18(100), 49(87.9), 31(58.2), 56(25.7)	
2	20.1	1.5	347(2)	15※(100), 14(12.1), 32(7.7), 18(5.5), 16(5.2)	31(100), 46(30.7)	
3	17.9	1.5	329	15※(100), 14(12.1), 18(9.4), 32(8.3), 30(8.0)	46(100), 15(40.1)	
4	24.3	2.5	345	30(100), 15(99.3), 16(68.5), 69(51.3), 56(35.9), 18(34.6), 46(29.5)		
5	27.7	1.5	343(1)	30※(100), 15(80.6), 14(15.2), 29(13.5), 18(4.9), 28(4.8), 44(4.1), 31(2.7), 45(2.4)	28(100), 16(15.6), 30(8.4)	
6	30.7	1.5	343(2)	15※(100), 61(97.6), 44(33.1), 30(26.6), 33(23.8), 60(20.7), 16(13.6), 14(13.0), 32(9.0), 46(8.0)	46(100), 29(19.9), 18(18.0), 45(14.3), 15(9.3), 28(4.7), 30(4.4), 31(2.1)	
7	22.4	2	359	15※(100), 30(51.4), 14(23), 61(17.3), 29(8.4), 48(8.0), 60(3.3)	15※(100), 46(22.5), 14(12.0), 33(4.5), 45(3.8), 31(3.7), 61(3.0), 29(2.7), 18(2.5)	
8	28.8.	1	375(1)	15※(100), 33(71.8), 16(46.9), 30(37.3), 32(16.4), 14(14.4), 17(10.8), 50(10.8), 58(9.7), 29(8.6)	18(100), 15(19.0), 49(11.2), 16(9.2), 33(9.1), 17(9.0), 29(8.6), 48(6.9)	
9	29.9	1	375(2)	15※(100), 30(57.1), 33(48.5), 48(30.9), 29(21.2), 14(11.3), 16(7.3), 32(6.1), 61(6.0), 18(5.5)	15※(100), 18(44.9), 33(23.4), 14(13.6), 46(4.0), 32(2.9), 17(2.8), 47(2.6), 48(2.1)	33(100), 30(20.7), 32(12.5)
10	29.3	1.5	391	30※(100), 15(80.4), 33(26.0), 48(23.8), 32(13.8), 17(9.3), 50(3.2), 28(3.1), 58(3.1), 61(2.9)	28※(100), 18(21.6), 43(6.7), 30(4.7), 17(4.2), 32(2.1), 31(1.9)	15(100), 50(26.3), 18(14.5), 14(10.2), 74(10.2), 60(9.6), 32(8.4), 36(6.1), 46(6.1)
11	23.1	1.5	373(1)	15※(100), 30(94.4), 29(24.7), 14(17.2), 18(8.3), 16(8.2), 28(4.2), 44(3.4)	28(100), 27(27.1), 56(19.4), 15(18.8), 58(8.5)	
12	26.0	1.5	373(2)	61※(100), 15(87.2), 44(33.0), 30(27.9), 60(22.2), 33(21.5), 16(19.7), 14(13.4), 31(7.9)	15(100), 43(42.4), 61(17.7), 16(17.7), 44(9.9), 31(9.3), 28(8.1), 33(7.2)	
13	34.2	1.5	373(3)	15※(100), 30(54.4), 29(10.3), 61(9.7), 48(4.7), 76(3.2), 60(2.4), 28(1.9)	15※(100), 46(20.1), 33(4.9), 45(3.0), 61(2.6), 29(2.0), 64(1.0)	46(100), 15(74.6), 18(38.7), 28(35.0), 74(13.8), 61(13.3), 17(10.2), 43(8.3), 30(6.5)
14	21.8	1.5	389(1)	15※(100), 30(63.0), 47(9.5), 18(6.2), 31(5.9), 46(5.8), 32(5.8), 61(1.6), 28(1.5)	15※(100), 33(35.8), 18(14.1), 32(8.1), 46(4.6)	18(100), 15(19.9), 17(18.4), 28(5.8), 31(5.8), 30(5.4), 49(4.7), 44(4.4), 43(4.2)
15	23.3	1.5	389(2)	15※(100), 30(92.8), 47(6.9), 60(5.9), 45(1.5), 32(1.3)	15※(100), 46(10.4), 32(3.6), 33(1.9), 17(1.3), 18(1.2), 29(1.0), 61(0.7), 30(0.6)	46(100), 15(36.6), 18(35.7), 28(17.3), 43(15.4), 45(7.0), 61(5.4)
16	26.5	1.5	389(3)	30※(100), 15(46.6), 28(5.6), 44(0.7), 74(0.7), 43(0.5)	28※(100), 15(14.4), 56(7.8), 74(5.2), 43(4.8), 30(4.0), 46(3.2)	15(11.7), 18(11.4), 61(8.3), 56(7.5)
17	29.7	1.5	389(4)	30※(100), 15(65.0), 33(37.7), 48(34.2), 29(27.3), 14, (16.7), 61(12.6), 47(11.4), 32(11.1), 60(3.6)	18(100), 31(51.0), 32(37.1), 15(28.5), 46(21.6), 17(17.1), 28(15.6), 30(11.5), 29(10.9), 60(8.7)	
18	36.6	1.5	389(5)	30※(100), 15(58.8), 32(19.5), 47(6.6), 60(2.2), 28(1.8), 61(1.8)	18※(100), 31(49.8), 32(31.1), 15(16.5), 28(12.8), 16(6.9), 30(4.5), 43(4.3), 61(3.4)	15(94.0), 28(85.7)
19	39.0	1.5	389(6)	15※(100), 30(75.0), 33(24.3), 14(21.6), 48(13.3), 29(12.3), 32(7.8), 61(4.9), 60(3.4)	15※(100), 14(20.8), 18(17.2), 17(6.6), 43(3.7), 33(3.1), 46(1.7), 61(1.5)	28(100), 15(49.2), 18(41.2), 43(27.1), 61(22.6)
20	24.6	1.5	405(1)	15※(100), 30(46.1), 47(4.5), 32(4.3), 16(2.9), 31(2.4), 33(2.4)	15※(100), 33(10.8), 17(6.1), 18(4.4), 32(4.2), 43(1.0), 30(0.7)	28(100), 18(10.0), 30(3.5), 43(2.4), 17(1.9), 48(1.8)

Table 3 (*Continued*)

No.	RT (min)	FA (V)	$[M+H]^+$ (*m/z*)	MS/MS loss (u) (%)	MS/MS/MS loss (u) (%)	MS/MS/MS/MS loss (u) (%)
21	26.3	1.5	405(2)	15※(100), 30(35.0), 32(5.5), 31(4.4), 60(0.7), 17(0.7), 61(0.6)	15※(100), 18(15.3), 33(1.1), 32(0.8), 30(0.4)	28(100), 18(50.9), 15(13.2), 46(10.5), 43(10.1), 61(7.6), 31(5.0), 17(3.3), 45(3.0)
22	32.2	1.5	405(3)	30※(100), 15(66.2), 32(18.7), 31(18.5), 17(15.8), 16(14), 14(13.9), 47(10.2), 33(3.1)	28※(100), 18(58.1), 17(21.4), 46(18.9), 15(16.7), 60(7.0), 48(6.8), 32(6.3)	33(100), 18(56.8), 30(42.6), 32(35.9), 15(33.6), 44(31.5), 16(31.0), 14(28.5)
23	36.0	1.5	405(4)	30※(100), 15(66.6), 32(13.2), 31(13.0), 47(7.7), 17(3.5)	28※(100), 18(20.4), 17(6.1), 31(1.6), 43(1.6), 46(1.5), 15(1.4), 30(1.0)	15(100), 18(23.8), 46(12.6), 61(9.7), 74(7.9), 30(7.1)
24	29.5	1	403	15※(100), 30(88.9), 61(2.8), 60(2.3), 14(2.3), 31(1.4), 47(1.1)	15※(100), 45(3.0), 32(1.4), 60(1.0), 17(0.8), 18(0.7), 30(0.5), 28(0.5)	46(100), 15(36.7), 18(28.1), 28(20.8), 45(20.4), 43(17.2)
25	24.1	1	419(1)	30※(100), 15(77.7), 33(6.2), 48(3.9), 31(2.6), 61(2.1), 18(1.5)	18※(100), 15(60.3), 28(48.4), 17(28.3), 33(14.5), 43(14.4), 30(12.8)	15(97.1), 14(60.3), 28(51.2), 29(50.2), 33(42.3), 46(27.6)
26	24.9	1	419(2)	15※(100), 30(71.4), 48(0.6), 33(4.2), 32(3.4), 47(3.0), 28(3.0), 46(1.4)	15※(100), 33(9.9), 31(6.4), 18(4.0), 32(2.9), 34(2.4), 49(2.1), 61(1.9)	15(100), 28(67.1), 16(51.6), 30(32.5), 18(31.7), 43(27.7), 33(18.4),
27	33.1	1	419(3)	15※(100), 30(52.7), 33(6.1), 31(5.3), 48(0.8)	15※(100), 17(15.9), 43(0.4), 32(0.3), 33(0.3)	28(100), 18(36.1), 15(19.6), 60(6.3), 33(3.6), 44(3.5), 45(3.3)
28	39.1	1	419(4)	30※(100), 15(78.0), 33(17.1), 48(7.4), 28(3.7), 45(1.3)	28※(100), 15(57.8), 18(52.8), 43(46.5), 46(25.8), 61(24.2), 14(15.7), 32(12.5), 33(11.1)	15(100), 33(32.5), 18(16.8), 28(11.7), 30(6.6), 46(6.0), 45(5.4)
29	31.5	1	433	30※(100), 15(99.4), 48(3.8), 31(3.7), 32(3.4), 47(2.7), 46(2.6), 33(1.6)	15※(100), 32(5.4), 30(4.7), 18(3.3), 60(1.6), 44(0.9)	15(100), 16(82.4), 30(64.1), 28(52.8), 18(41.2), 32(37.8), 43(21.8), 46(18.6), 58(17.6), 33(14.5)

$[M+H]^+$ represents the *m/z* of the protonated molecule. Loss (u) (%) represents the lossing fragments. The product ions tag with "※" represents precursor-ion for next stage MS.

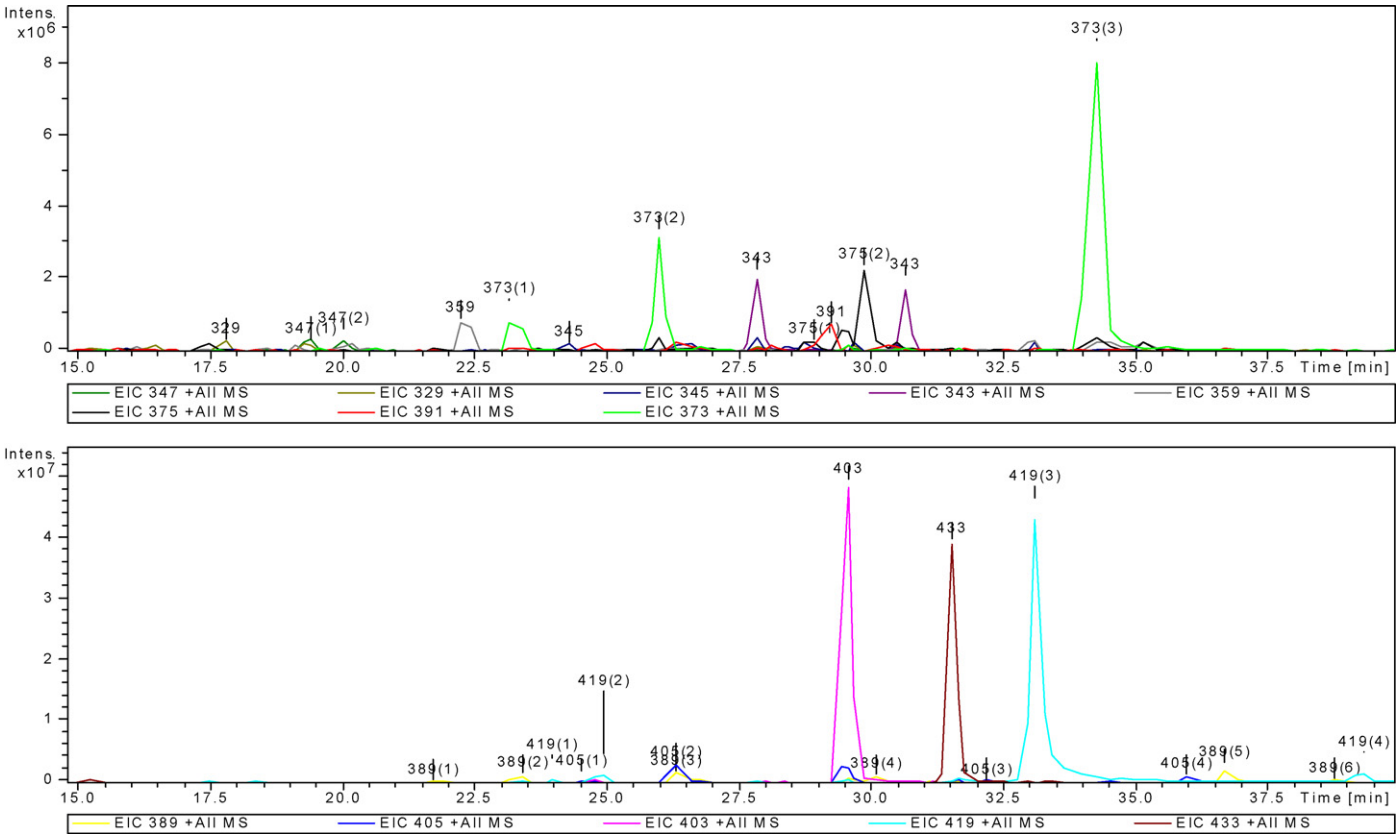

Fig. 6. The EIC MS peaks of all possible PMFs (the peaks were exhibited in two figures for clarity).

compounds existing in *F. aurantii* can be designed in advance. After screening these MWs with EIC method, 29 possible PMFs compounds in *F. aurantii* were detected (see Table 2 and Fig. 6). It showed that most EIC-MS peaks were too weak to form visible peaks in TIC MS spectra except *m/z* 403, *m/z* 433, *m/z* 419(3) and *m/z* 373(3). Meanwhile, some EIC-MS peaks such as *m/z* 405(2) and *m/z* 389(3) had nearly the same retention time (RT) and could not be detected simultaneously in TIC mode. These phenomena confirmed that EIC method was effective for preliminary screening of target compounds in highly complex matrix.

3.4. Verification with MS^n spectra

All candidates for PMFs were firstly screened by EIC-MS method, but further verification with their MS^n information was still needed. In MS^n experiments, the FA was set from 1 to 4 V (1, 1.5, 2, 2.5, 3, 3.5, and 4 V) to obtain the optimal MS^n information which was served for verification of PMFs by comparing with MS^n "fingerprint" obtained from SIN and TAN. The MS^n information of the 29 target compounds (see Table 3) had three distinct characters which were accord with the "fingerprint" of PMFs obtained by SIN and TAN: (1) the base and secondary peaks in MS^2 spectra were mainly radical cations from the loss of one or two methyl groups ($CH_3^{\bullet}$) except *m/z* 373(2) for base peak and *m/z* 347(1), *m/z* 347(2), *m/z* 329, *m/z* 343(2), *m/z* 375(1) for secondary peaks; (2) other main product-ions were diagnostic fragments of SIN and TAN from the loss of 15, 29, 30, 33, 43, 46, 61, 14, and 16; (3) beside those diagnostic fragments for PMFs, additional product-ions include fragments corresponding to the neutral loss of 18, 28 and 44. Therefore, the 29 compounds were preliminarily be verified as PMFs among which *m/z* 373(2) and *m/z* 373(3) were identified as SIN and TAN since they had identical RTs and MS^n information. For other compounds, they could only be verified as PMFs, but the exact position of substituent groups could not be confirmed.

4. Conclusion

This study was to screen and characterize PMFs from *F. aurantii* by MS method, which was achieved with diagnostic MS^n "fingerprint" and EIC-MS method. The diagnostic MS "fingerprint" of PMFs was obtained from standards SIN and TAN through CID-MS experiments and was adopted as a basis for further characterization of PMFs in candidate compounds screened through EIC method by MWs. Protonated PMFs produced specific fragmentation from the loss of 15, 29, 30, 33, 43, 46, and 61, which formed characteristic MS^n "fingerprint" using a PI-APCI MS^n. EIC-MS method was validated to be an effective method for screening target PMFs with designed MWs in highly complex mixtures. Twenty-nine PMFs in *F. aurantii* were characterized preliminarily and two of them were identified as SIN and TAN exactly by comparing their MS^n information with the MS^n "fingerprint". It indicates that LC APCI-MS/MS is a powerful tool for the screening and characterization of PMFs species in complex matrix.

Acknowledgements

This work was supported by "Key project of National Science Foundation of China (20235020)" and "Key Project of Knowledge Innovation Program of Chinese Academy of Sciences (KGCX2-SW-213)".

References

[1] Y. Satoh, S. Tashiro, M. Satoh, Y. Fujimoto, J.Y. Xu, T. Ikekawa, Yakugaku Zasshi 116 (1996) 244–250.
[2] Y.T. Huang, G.F. Wang, C.F. Chen, C.C. Chen, C.Y. Hong, M.C. Yang, Life Sci. 57 (1995) 2011–2020.
[3] X.W. Zhao, J.X. Li, Z.R. Zhu, D.Q. Sun, S.C. Liu, Chin. Med. J. (Engl). 102 (1989) 91–93.
[4] D.Y. Zhou, Q. Xu, X.Y. Xue, F.F. Zhang, X.M. Liang, J. Pharm. Biomed. Anal. 42 (2006) 441–448.
[5] H. Smith, in: K. Mitrakos, W. Shropshire (Eds.), Phytochrom, Academic Press, London, 1972, pp. 433–434.
[6] S. Kobayashi, S. Tanabe, Int. J. Mol. Med. 17 (2006) 511–515.
[7] Y.Q. Wu, C.H. Zhou, J. Tao, S.N. Li, Life Sci. 78 (2006) 2689–2696.
[8] M.A. Anagnostopoulou, P. Kefalas, E. Kokkalou, A.N. Assimopoulou, V.P. Papageorgiou, Biomed. Chromatogr. 19 (2005) 138–148.
[9] S. Kawaii, Y. Tomono, E. Katase, K. Ogawa, M. Yano, Biosci. Biotechnol. Biochem. 63 (1999) 896–899.
[10] J. Yanez, V. Vicente, M. Alcaraz, J. Castillo, O. Benavente-Garcia, M. Canteras, J.A. Teruel, Nutr. Cancer 49 (2004) 191–199.
[11] G.K. Jayaprakasha, P.S. Negi, S. Sikder, L.J. Rao, K.K. Sakariah, Z. Naturforsch [C]. 55 (2000) 1030–1034.
[12] R.W. Li, A.G. Theriault, K. Au, T.D. Douglas, A. Casaschi, E.M. Kurowska, R. Mukherjee, Life Sci. 79 (2006) 365–373.
[13] E. de Rijke, H. Zappey, F. Ariese, C. Gooijer, A.J. Udo, Chromatogr. A. 984 (2003) 45–58.
[14] A.S. Abdelaaty, F. Cuyckens, W. Wang, K.A. Abdel-Shafeek, H.A. Husseiny, S. Apers, S. Van Miert, L. Pieters, J.V. Arnold, M. Claeys, Rapid Commun. Mass Spectrom. 19 (2005) 2172–2178.
[15] M. Satterfield, J.S. Brodbelt, J. Am. Soc. Mass Spectrom. 12 (2001) 537–549.
[16] M. Pikulski, J.S. Brodbelt, J. Am. Soc. Mass Spectrom. 14 (2003) 1437–1453.
[17] F. Ferreres, R. Llorach, A. Gil-Izquierdo, J. Mass Spectrom. 39 (2004) 312–321.
[18] Ulla Justesen, J. Mass Spectrom. 36 (2001) 169–178.
[19] N. Fabre, I. Rustan, E. de Hoffmann, J. Quetin-Leclercq, J. Am. Soc. Mass 12 (2001) 707–715.